(14) AMMRC-TR-78-24

AD

(6) PROBABILITY BASED FRACTURE MECHANICS FOR IMPACT PENETRATION DAMAGE,

(10) THOMAS P. RICH, PETER G. TRACY, LOUIS R. TRAMONTOZZI, JIRO ADACHI, MILO BENICEK, ALAN H. KATZ, and WILBERT J. FOSTER

MECHANICS OF MATERIALS DIVISION

(16) 1L162105AH84 (17) pp

June 1978 (11) 10 Sep 76

(12) 29 p.

Approved for public release; distribution unlimited.

ARMY MATERIALS AND MECHANICS RESEARCH CENTER
Watertown, Massachusetts 02172

403 105

The findings in this report are not to be construed as an official Department of the Army position, unless so designated by other authorized documents.

Mention of any trade names or manufacturers in this report shall not be construed as advertising nor as an official indorsement or approval of such products or companies by the United States Government.

DISPOSITION INSTRUCTIONS

Destroy this report when it is no longer needed.
Do not return it to the originator.

UNCLASSIFIED

SECURITY CLASSIFICATION OF THIS PAGE (When Data Entered)

REPORT DOCUMENTATION PAGE		READ INSTRUCTIONS BEFORE COMPLETING FORM
1. REPORT NUMBER AMMRC TR 78-24	2. GOVT ACCESSION NO.	3. RECIPIENT'S CATALOG NUMBER
4. TITLE (and Subtitle) PROBABILITY BASED FRACTURE MECHANICS FOR IMPACT PENETRATION DAMAGE		5. TYPE OF REPORT & PERIOD COVERED 6. PERFORMING ORG. REPORT NUMBER
7. AUTHOR(s) Thomas P. Rich, Peter G. Tracy, Louis R. Tramontozzi, Jiro Adachi, Milo Benicek, Alan H. Katz, and Wilbert J. Foster		8. CONTRACT OR GRANT NUMBER(s)
9. PERFORMING ORGANIZATION NAME AND ADDRESS Army Materials and Mechanics Research Center Watertown, Massachusetts 02172 DRXMR-TM		10. PROGRAM ELEMENT, PROJECT, TASK AREA & WORK UNIT NUMBERS D/A Project: 1L162105AH84 AMCMS Code: 612105.H840011 Agency Accession: DA OG4670
11. CONTROLLING OFFICE NAME AND ADDRESS U. S. Army Materiel Development and Readiness Command, Alexandria, Virginia 22333		12. REPORT DATE June 1978 13. NUMBER OF PAGES 24
14. MONITORING AGENCY NAME & ADDRESS(if different from Controlling Office)		15. SECURITY CLASS. (of this report) Unclassified 15a. DECLASSIFICATION/DOWNGRADING SCHEDULE

16. DISTRIBUTION STATEMENT (of this Report)

Approved for public release; distribution unlimited.

17. DISTRIBUTION STATEMENT (of the abstract entered in Block 20, if different from Report)

18. SUPPLEMENTARY NOTES

Published in International Journal of Fracture, vol. 13, no. 4, August 1977, p. 409-430

19. KEY WORDS (Continue on reverse side if necessary and identify by block number)

Fracture
Probability
Impact
Damage

20. ABSTRACT (Continue on reverse side if necessary and identify by block number)

(SEE REVERSE SIDE)

DD FORM 1 JAN 73 1473 EDITION OF 1 NOV 65 IS OBSOLETE

UNCLASSIFIED

SECURITY CLASSIFICATION OF THIS PAGE (When Data Entered)

78 11 10 052

Block No. 20

ABSTRACT

This paper presents a new method for assessing the residual strength of structural components which have sustained impact penetration damage. The method is based upon the application of the Weibull probability density function to account for the significant scatter in residual strengths which result from the random nature of impact damage detail (cracks, holes, and spall surfaces). To measure the extent of an impact damage pattern, a new parameter is presented which is based upon the solution for an inclined crack in a uniaxial tension field and an experimentally obtained fracture criterion for mixed mode crack configurations. Test results are presented for residual strengths of machined damage specimens to ascertain the statistical nature which arises from extreme damage detail, smooth holes and sharp cracks. Finally, probability of failure curves are given for both machined (7075-T6) and impact damage (7075-T6 and 2024-T81) in aluminum uniaxial tension panels.

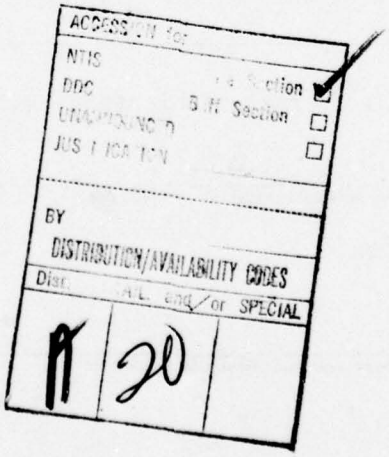

Reprinted through courtesy of Sijthoff and Noordhoff from
International Journal of Fracture, Vol. 13, No. 4, August 1977
Noordhoff International Publishing – Alphen aan den Rijn
Printed in The Netherlands

Probability based fracture mechanics for impact penetration damage

T.P. RICH, P.G. TRACY, L.R. TRAMONTOZZI, J. ADACHI, M. BENICEK, A.H. KATZ and W. FOSTER

Mechanics Research Laboratory, Army Materials and Mechanics Research Center, Watertown, Massachusetts 02172, *USA*

(Received September 16, 1976; in revised form February 25, 1977)

ABSTRACT

This paper presents a new method for assessing the residual strength of structural components which have sustained impact penetration damage. The method is based upon the application of the Weibull probability density function to account for the significant scatter in residual strengths which result from the random nature of impact damage detail (cracks, holes, and spall surfaces). To measure the extent of an impact damage pattern, a new parameter is presented which is based upon the solution for an inclined crack in a uniaxial tension field and an experimentally obtained fracture criterion for mixed mode crack configurations. Test results are presented for residual strengths of machined damage specimens to ascertain the statistical nature which arises from extreme damage detail, smooth holes and sharp cracks. Finally, probability of failure curves are given for both machined (7075-T6) and impact damage (7075-T6 and 2024-T81) in aluminum uniaxial tension panels.

1. Introduction

The possibility of impact damage during the operational life of a structure can establish the necessity for a fracture mechanics, residual strength assessment even when accurate NDT and inspection procedures indicate highly safe performance under ordinary operating conditions. Such damage can obviously arise for structures operating under the risk of impact from natural or ballistic projectiles. Other situations exist where impact damage can occur from common operational accidents such as a back-hoe striking a pressurized pipe line while digging in an open field. Various examples throughout the literature [1–6] indicate that design engineers are aware of the problem and have attempted to include rational consideration of impact damage in the design process. The past approaches as summarized in [7] have been attempts to estimate the residual strength of an impact damaged structure from a deterministic mechanics/empirical viewpoint by utilizing simplified concepts from conventional fracture mechanics. Thus, procedures have evolved to assess the degree of damage in terms of some "effective flaw size" and relate it to a critical operational load through an "impact damage fracture toughness".

This paper presents an approach which acknowledges that impact damage is an extremely complex degradation of a structural component. For a given set of impact conditions: projectile, velocity, angle of impact, structural configuration, and materials, the detailed nature and extent of damage is beyond prediction by the current state of solid mechanics. Moreover, because of the apparently random nature of the damage detail (cracks, holes, and spall surfaces), the proposed approach for the evaluation of residual strength is based upon a statistical rather than a deterministic foundation. In this manner a statistical probability distribution is utilized to account for the scatter which is apparent in the residual strengths of impact damaged

components as a result of the insensitivity to the damage detail of available damage measures. A methodology is established wherein one employs a new fracture mechanics based parameter, d_{im}, to estimate the extent of damage from a specific impact penetration; then through a corresponding statistical function determines the probability of failure as a function of the operational load for a structural component containing d_{im}.

The following sections present the basis for d_{im}, application of the Weibull distribution function to correlate the probability of failure with d_{im}, and a demonstration of the probability approach in conjunction with residual strength data for high strength aluminum specimens containing machined, controlled damage (cracks and holes) and ones containing ballistic impact damage.

2. Impact damage measure

Before an evaluation of residual strength can be made, it is necessary to measure the extent and nature of damage resulting from a given impact penetration. Figure 1 illustrates a typical impact damage configuration as might result from an impact penetration. Note that in general a complex damage detail arises from which a resulting mechanism of fracture propagation will initiate when a critical load is

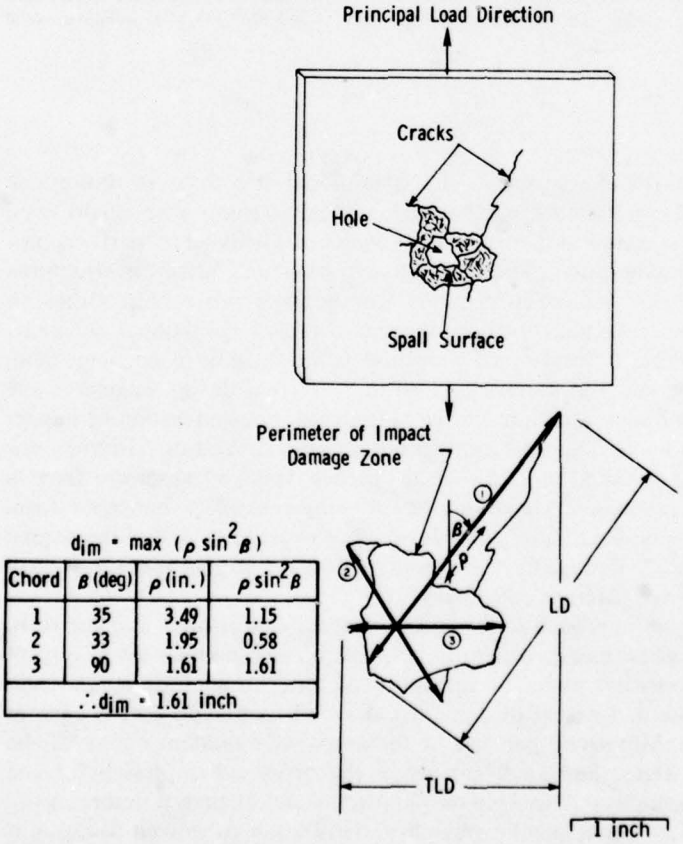

$d_{im} = \max(\rho \sin^2 \beta)$

Chord	β (deg)	ρ (in.)	$\rho \sin^2 \beta$
1	35	3.49	1.15
2	33	1.95	0.58
3	90	1.61	1.61
$\therefore d_{im} = 1.61$ inch			

Figure 1. Measures of impact penetration damage.

reached in the structure. References [8 and 9] provide definitions of the two heretofore established measures of impact damage. The first is the lateral damage, LD, defined as the greatest dimension characteristic of the extent of detectable impact damage including through-hole, cracks, and spall surfaces. This measurement is independent of load orientation. In contrast the second measure, termed the transverse lateral damage, TLD, is the maximum damage as measured perpendicular to the direction of principal loading.

TLD appears to have been the more successful parameter for correlation with residual strengths from all reports in the literature. However, one can observe that TLD as well as any simplified damage parameter is insensitive to the smoothness (hole) versus the sharpness (cracks) which may result from a given impact damage situation. Even for the cases where cracks are certain to be associated with impact damage, Fig. 2 illustrates a weakness in TLD. Here is shown a series of extreme cases of damage detail where cracks are oriented at varying angles to the principal load; the critical load is shown to differ greatly with crack angle in test data described in a later section; yet TLD is constant. To enable some influence of this orientation of damage

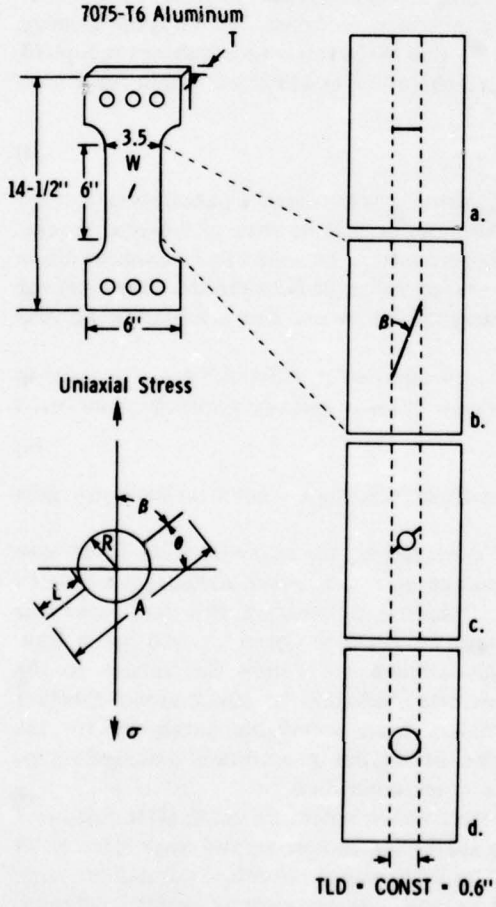

Figure 2. Specimen configurations for machined, controlled damage specimens.

to be accurately incorporated into an impact damage measure, the following new measure has been devised.

The stress intensity factors for a crack inclined at some angle, β, (Fig. 2b) to the principal load direction in uniaxial tension is known as [10]

$$K_I = \sigma\sqrt{\pi\rho/2}\sin^2\beta$$
$$K_{II} = \sigma\sqrt{\pi\rho/2}\sin\beta\cos\beta \quad (1)$$

where ρ is the total crack length. Fracture tests of structural materials under mixed mode conditions [11, 12] show that at least for angles of β ranging from twenty to ninety degrees, the following relationship provides a reasonable fracture criterion for many applications.

$$K_I^2 + K_{II}^2 = C_o^2 \quad (2)$$

where C_0 is the conventional fracture toughness.

Substitution of (1) into (2) leads to the following relationship between fracture stress, σ_c, and damage parameters ρ and β.

$$\sigma_c = C_0\sqrt{2/\pi}(\rho\sin^2\beta)^{-\frac{1}{2}} \quad (3)$$

This equation, which was derived for a single inclined crack, suggests a parameter, d_{im}, which can be extended for use as a measure of impact penetration damage. Specifically, d_{im} is defined to be the maximum value of the term in parentheses in Eqn. (3) for the set of all possible inclined cracks which can be constructed within the impact damage zone.

$$d_{im} = \text{Max}\,(\rho\sin^2\beta) \quad (4)$$

As illustrated in Fig. 1, to measure d_{im} from a given impact penetration damage pattern, a perimeter is first established around the detectable zone of damage: cracks, hole and/or spall surface. The impact damage measure becomes the maximum value of a damage chord times the square of the sine of the angle between the chord and the principal load direction as all chords characteristic of the damage pattern are examined within the perimeter.

Note that for most instances of normal, as opposed to oblique, impact damage in nearly isotropic materials, the resulting damage is fairly radially symmetric and often

$$\text{TLD} \cong \text{Max}\,(\rho\sin\beta) \cong d_{im} \quad (5)$$

where $\beta \cong 90°$. For that case a good statistical correlation between residual strengths and TLD can be anticipated.

However, for cases of highly skewed damage patterns resulting from an oblique impact or a highly anistropic material/damage response, d_{im} more accurately measures the extent of damage for use in a residual strength determination. It is postulated that while neglecting some possible crack damage interactions not accounted for in Eqn. (1), d_{im} includes a rational variation with damage orientation and relates to the fracture stress, σ_c, as a square root "flaw size" inherent to conventional fracture mechanics toughness parameters. This makes it an acceptable parameter for the statistical correlation of residual strengths of impact penetration damaged components, especially when the strengths are crack-controlled.

Note that d_{im} does not include parameters which reflect material, plate thickness or certain aspects of damage detail such as sharpness, or hole versus crack size. All of these factors influence residual strength. The influence of structural parameters such as material and thickness can be isolated by selective grouping of residual strength data before statistical analysis is performed. The influence of damage detail not

included in d_{im} is accounted for in the spread of the statistical distribution of residual strengths.

3. Residual strength via Weibull distribution

The strength of any material is known to be a function of somewhat random variables: manufacturing flaws, impurities, voids, process variations, etc. Therefore, the strength of any given material is more accurately represented by a statistical distribution than by a single average handbook value. Freudenthal [13] employed this philosophy in his investigation of the ultimate strengths of aircraft components without impact damage. Various aircraft components and substructures were tested to failure under loading conditions similar to what they would experience in operation. This raw strength data was then statistically analyzed employing various probability distributions to represent the observed scatter. It was found that the Weibull distribution function [14] provided the best representation of his residual strength data. This distribution function is written as

$$L(z) = \exp\left[-(z/\nu)^{\eta}\right] \tag{6}$$

where $L(z)$ is the probability of component survival,
$z = \sigma/\sigma_{\mathrm{ULT}}$, the loading stress/design ultimate stress, and
ν, η are the empirical parameters for Weibull fit.

Two important facts are evident when considering Freudenthal's statistical results. First, the design ultimate stress, σ_{ULT}, is that averaged strength level measured under the considered type of loading. For example, a component under tension would be normalized to the ultimate tensile strength of the material, one under torsion – the shear strength, etc. Second, "the distribution of the ultimate strength of the test specimens can be considered to represent a single population irrespective of the type of structures tested and its mode of failure, as long as this failure can be classified as ultimate [13]". This postulate is born of necessity to a degree because of the cost of replication and the accompanying scarcity of ultimate strength data for aircraft components. More data is required to prove the validity of the postulate; the resulting distribution obtained by Freudenthal will be compared in a later section to some current residual strength data for tension specimens containing no machined or impact penetration damage. It provides a limiting case for the statistical distributions of impact penetration damaged components as d_{im} approaches zero.

To evaluate the residual strength of impact penetration damaged components, an extension of the Freudenthal approach for undamaged ones is made. Whereas in the "undamaged" case, all flaw sizes are of a microscopic order of magnitude, i.e. grain sizes, etc., impact damage can introduce a much more extensive flaw which then controls the residual strength. The resulting residual strength distributions for the impact damaged components become a set of Weibull functions; each one established for a given d_{im}. The following development outlines the statistics for determining the Weibull probability of failure function from a given set of residual strength data collected from specimens with a constant d_{im}.

Given that the probability of survival of a component containing d_{im} under an operational loading stress, σ, is provided by (6), the probability of failure is

$$\begin{aligned} P(z) &= 1 - L(z) \\ &= 1 - \exp\left[-(z/\nu)^{\eta}\right] \end{aligned} \tag{7}$$

Note that at this stage the theory is strictly applicable to a uniaxial stress in the region of impact damage.

To isolate ν and η, form the expression

$$\ln\left\{\ln\left[\frac{1}{1-P(z)}\right]\right\} = \ln\left\{\ln\left[\exp\left(z/\nu\right)^{\eta}\right]\right\}$$
$$= \eta \ln\left(z/\nu\right)$$
$$= \eta \ln z - \eta \ln \nu \tag{8}$$

It can be seen that this last expression has the form of a straight line, $y = mx + b$, where

$$y = \ln\left\{\ln\left[\frac{1}{1-P(z)}\right]\right\}$$
$$x = \ln z$$
$$b = -\eta \ln \nu$$
$$m = \eta \tag{9}$$

This relationship provides a means for the determination of ν and η from a set of k residual strength data specimens. In the current work the data will be the stresses, σ_i, in uniaxial tension at which specimens containing damage, d_{im} = const, failed by fracture. From this data the ratios, $z_i = \sigma_i/\sigma_{\mathrm{ULT}}$, can be formed. The next step is to order in ascending fashion and renumber the z_i's such that z_1 has the smallest and z_k the largest value.

For each of the specimens the values of

$$x_i = \ln z_i, \quad y_i = \ln\left\{\ln\left[\frac{1}{1-P(z_i)}\right]\right\} \tag{10}$$

are then calculated, where the cumulative probability of failure of any given specimen at σ_i is computed from the finite data sample as

$$P(z_i) = i/k \tag{11}$$

In order to represent the data by a Weibull distribution, the resulting test values, (x_i, y_i) are fit to a straight line using least squares. Note that the definitions of z and $P(z_i)$ insure that the test values will be on a single, but perhaps curved, line. The least squares fit determines the straight line which most closely approximates the test values line. For a set of best fit parameters (m_0, b_0), Eqns. (9) are used to determine the corresponding Weibull parameters.

$$\eta = m_0$$
$$\nu = \exp\left(-b_0/m_0\right) \tag{12}$$

This algorithm can be easily programmed for a digital computer. An alternate means of finding the best Weibull fit for a set of residual strength data is through the use of probability paper, which in essence is a graphical procedure which duplicates the mathematical algorithm presented above [15].

Close inspection of the Weibull distribution function leads to a physical interpretation for ν and η. ν can be considered as indicative of the average strength ratio for a given set of residual strength data, while η is a measure of the dispersion of strength values. Large values of η indicate a tight statistical distribution with correspondingly low scatter.

Once the values of ν and η have been determined for a given material under uniform tension and containing impact damage, d_{im}, Eqn. (7) provides the probability

of failure for any single value of loading tensile stress. The derivative function of (7) is the probability density function for the Weibull distribution:

$$f(z) = \mathrm{d}P(z)/\mathrm{d}z$$

$$= \exp(\eta/\nu)(z/\nu)^{\eta-1}[-(z/\nu)^{\eta}] \tag{13}$$

It is this function which can be used to represent the strength distribution in a conventional structural reliability analysis where the operational load is characterized by a spectrum rather than a single peak value [16]. Figure 3 shows the probability of failure in this instance to be the intersecting area between the anticipated operational load distribution and the Weibull strength distribution corresponding to the appropriate value of d_{im}.

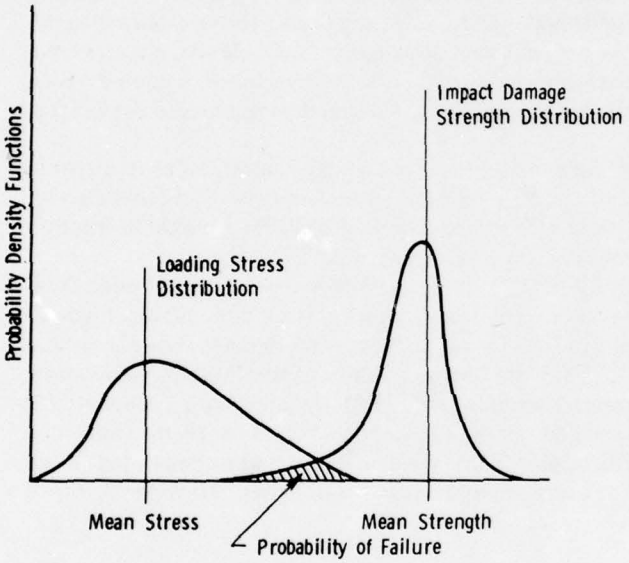

Figure 3. Schematic of structural reliability analysis.

Finally, in all statistical applications the question arises as to the degree which the assumed distribution function fits a given set of data. In addition to the past evidence [13, 14] which demonstrates the applicability of the Weibull probability function to "weakest link" type of physical phenomena, typified by impact damage residual strengths, a positive check should be made for each correlation by a goodness-of-fit test. In the current work the Chi-squared test was used to establish the degree of correlation.

4. Machined controlled damage

To gain insight into the sensitivity of the measures of impact damage with respect to the extreme forms of damage detail, sharp cracks to smooth holes, and to establish a statistical base for residual strength under closely controlled damage for comparison to the results from tests with impact damage of the same order, a series of residual strength tests were performed with 7075-T6 aluminum specimens as shown in Fig. 2. These tests were run under uniaxial tension and encompassed three specimen

thicknesses, 0.050, 0.100, and 0.250 inch, to explore the fracture response from near plane stress to near plane strain conditions. The raw data from these tests are presented in Tables I to VI where the data has been grouped according to the form of damage detail and nominal values of d_{im}. Three primary forms of damage have been investigated: (1) NO DAMAGE where no machined damage is present and failure is controlled by the inherent material weaknesses which determine the ultimate tensile strength; (2) SMOOTH DAMAGE where failure is initiated at a smooth machined hole; (3) SHARP DAMAGE where failure is initiated at sharp crack tips. Six nominal values of d_{im} were employed: 0.0″; 0.593″ – SMOOTH; 0.160″, 0.320″, 0.450″, and 0.630″ – SHARP.

All of the cracked specimens were machined such that the rolling direction of the material was parallel to the orientation of the crack. In this manner each crack tip lay in a similar field of anisotropy with respect to the material properties. The cracks were produced by an electrical discharge machining process which resulted in narrow slots approximately 0.006″ wide and with tip radii on the order of 0.001″. The slot lengths were intentionally made 0.010″ short of the desired final crack lengths. The remaining 0.010″ crack tip length was then made under high cycle fatigue with the load normal to the crack. The fatigue crack lengths were monitored by a closed circuit television system; the resulting total crack lengths for each specimen are reported as measured. A more detailed description and assessment of the crack producing and monitoring process is available [17].

For both the no damage specimens and those with only smooth holes, the rolling direction was established perpendicular to the applied tensile load. The failure stress in tension, σ_c, for all specimens was determined from the peak tensile load at fracture and the actual width and thickness of the specimen, W and T.

The values of σ_c from each table were utilized along with σ_{ULT} as obtained from the no damage results of Table I for a statistical analysis at each nominal d_{im}. Figure 4 presents the probability of failure curves for all of the SHARP damage data along with the no damage curve for comparison. Note how the values of the Weibull parameters, (ν, η), from the current no damage results, (1.005, 35.0) compare with Freudenthal's [13] parameters for the undamaged aircraft components, (0.96, 19.0). Both distributions possess a ν value which is near unity since the z_i's were computed based upon a normalization by the average undamaged strengths. However, the η

TABLE I
Residual strengths 7075-T6 machined, controlled damage.†

	Nominal $d_{im} = 0.0$					No damage		
No.	A	L	R	W	T	β	d_{im}	σ_c*
241				3.503	0.048		0.0	82073.
242				3.503	0.047		0.0	87463.
243				3.502	0.048		0.0	85070.
244				3.503	0.047		0.0	89285.
245				3.502	0.048		0.0	83880.
246				3.502	0.047		0.0	83843.
247				3.501	0.048		0.0	80929.
248				3.503	0.047		0.0	89285.
249				3.500	0.047		0.0	85714.

* σ_{ULT} = average σ_c = 85282.

† All dimensions of length in the tables are inches. (Refer to Fig. 2.) All angles are given in degrees, stresses in psi. No entry in a column indicates no damage characterized by the column heading existed in the given specimen.

TABLE II
Residual strengths 7075-T6 machined, controlled damage.

	$d_{im} = 0.593$					SMOOTH DAMAGE		
No.	A	L	R	W	T	β	d_{im}	σ_c
281			0.2965	3.504	0.048		0.593	64212.
282			0.2965	3.504	0.047		0.593	65579.
284			0.2965	3.500	0.048		0.593	67857.
285			0.2965	3.500	0.048		0.593	64881.
286			0.2965	3.500	0.047		0.593	67477.
288			0.2965	3.500	0.048		0.593	67262.
289			0.2965	3.500	0.048		0.593	67857.
209			0.2965	3.500	0.101		0.593	68175.
210			0.2965	3.500	0.101		0.593	67893.
212			0.2965	3.500	0.100		0.593	67893.
213			0.2965	3.500	0.100		0.593	69429.
214			0.2965	3.500	0.100		0.593	68571.
215			0.2965	3.500	0.100		0.593	68571.
217			0.2965	3.500	0.100		0.593	68000.
218			0.2965	3.500	0.100		0.593	68286.
68			0.2965	3.505	0.255		0.593	65341.
69			0.2965	3.512	0.255		0.593	64764.
70			0.2965	3.510	0.255		0.593	65024.
72			0.2965	3.505	0.255		0.593	66012.
73			0.2965	3.510	0.254		0.593	64607.
74			0.2965	3.515	0.255		0.593	64262.
75			0.2965	3.510	0.255		0.593	65024.
76			0.2965	3.505	0.255		0.593	67131.

TABLE III
Residual strengths 7075-T6 machined, controlled damage.

	Nominal $d_{im} = 0.160$					SHARP DAMAGE		
No.	A	L	R	W	T	β	d_{im}	σ_c
277	2.406			3.500	0.049	15.	0.161	52478.
278	2.375			3.500	0.048	15.	0.159	57857.
297	0.640	0.169	0.1510	3.500	0.051	30.	0.160	66106.
298	0.620	0.159	0.1510	3.500	0.050	30.	0.155	65143.
206	2.390			3.500	0.100	15.	0.160	56571.
207	2.375			3.500	0.100	15.	0.159	59429.
226	0.670	0.184	0.1510	3.500	0.100	30.	0.168	65143.
42	0.660			3.500	0.240	30.	0.165	65000.
43	0.650			3.496	0.255	30.	0.162	60237.
65	2.406			3.505	0.254	15.	0.161	51220.
66	2.437			3.495	0.255	15.	0.163	55542.
67	2.437			3.497	0.252	15.	0.163	54468.
97	0.640	0.169	0.1510	3.501	0.253	30.	0.160	60965.
98	0.655	0.177	0.1510	3.497	0.254	30.	0.164	63496.
99	0.637	0.168	0.1510	3.497	0.252	30.	0.159	61277.
143	2.345	0.782	0.3905	3.498	0.254	15.	0.157	60102.
144	2.366	0.793	0.3905	3.497	0.251	15.	0.158	62660.
145	2.330	0.775	0.3905	3.500	0.255	15.	0.156	62073.
147	2.360	0.790	0.3905	3.500	0.255	15.	0.158	61849.

TABLE IV
Residual strengths 7075-T6 machined, controlled damage.

	Nominal $d_{im} = 0.320$				SHARP DAMAGE			
No.	A	L	R	W	T	β	d_{im}	σ_r
274	1.300			3.496	0.051	30.	0.325	53170.
275	1.265			3.500	0.050	30.	0.316	54171.
203	1.250			3.503	0.101	30.	0.312	48332.
205	1.234			3.504	0.100	30.	0.308	49087.
33	0.656			3.496	0.241	45.	0.328	52105.
34	0.640			3.505	0.254	45.	0.320	47851.
35	0.656			3.495	0.252	45.	0.328	51775.
36	0.625			3.497	0.253	45.	0.312	50184.
37	0.655			3.497	0.253	45.	0.328	49845.
38	0.656			3.495	0.251	45.	0.328	46851.
39	0.679			3.498	0.253	45.	0.340	48136.
40	0.656			3.500	0.252	45.	0.328	48299.
57	1.255			3.500	0.253	30.	0.314	51904.
58	1.220			3.501	0.253	30.	0.305	48095.
59	1.255			3.503	0.253	30.	0.314	47878.
60	1.230			3.500	0.255	30.	0.308	51092.
61	1.235			3.500	0.255	30.	0.309	49748.
62	1.275			3.500	0.254	30.	0.319	46682.
63	1.290			3.500	0.254	30.	0.322	49494.
64	1.240			3.496	0.255	30.	0.310	50590.
94	0.712	0.145	0.211	3.503	0.251	45.	0.356	50497.
95	0.686	0.132	0.211	3.500	0.253	45.	0.343	54884.
96	0.680	0.129	0.211	3.501	0.252	45.	0.340	52139.
128	1.320	0.262	0.398	3.501	0.253	30.	0.330	56901.
129	1.228	0.216	0.398	3.500	0.249	30.	0.307	61274.
131	1.230	0.217	0.398	3.500	0.250	30.	0.308	62857.
132	1.225	0.215	0.398	3.501	0.251	30.	0.306	60313.
133	1.242	0.098	0.523	3.500	0.253	30.	0.310	56917.
134	1.227	0.090	0.523	3.500	0.253	30.	0.307	56917.
136	1.227	0.090	0.523	3.500	0.254	30.	0.307	57368.
137	1.244	0.099	0.523	3.500	0.252	30.	0.311	56463.

parameters indicate a much larger scatter in the Freudenthal test data than was present in the controlled no-damage tensile tests. The larger scatter in Freudenthal's data may be attributed to his postulate for combining residual strengths from failure tests under different kinds of loading.

One can see from Fig. 4 that a structural engineer can assess the probability of failure of a component with machined damage given an estimate of the principal loading stress and the designed-for damage measure, d_{im}. Note that as the degree of damage increases the probability curves shift towards the left. This is consistent with the concept that, at a given load level, the probability of failure increases with the degree of damage; a concept which will be seen to carry over into impact damage probability curves.

Figure 5 shows how the type of damage detail is reflected through the probability curves. The two groups have roughly the same d_{im} where in fact the smooth damage is greater than the sharp. However, the sharp crack controlled damage curve is located significantly to the left of the smooth stress concentration controlled damage curve. This demonstrates the importance of one aspect of damage detail, smoothness versus sharpness, and is useful in interpreting the scatter of actual impact damage residual strengths. The degree to which any given set of impact damage patterns is characterized by smoothness or sharpness depends upon the exact damage detail and is therefore directly influenced by the impact conditions including the energy level of the impact phenomenon.

The effect of specimen thickness is also shown by a shift in the probability

TABLE V
Residual strengths 7075-T6 machined, controlled damage.

	Nominal $d_{im} = 0.450$					SHARP DAMAGE		
No.	A	L	R	W	T	β	d_{im}	σ_c
265	0.875			3.499	0.051	45.	0.438	53797.
267	0.880			3.498	0.050	45.	0.440	55575.
268	0.880			3.497	0.050	45.	0.440	55591.
269	0.890			3.497	0.049	45.	0.445	56025.
270	0.895			3.500	0.050	45.	0.448	54514.
271	0.885			3.496	0.049	45.	0.442	56041.
272	0.895			3.496	0.050	45.	0.448	52860.
273	0.880			3.496	0.050	45.	0.440	54062.
293	0.640	0.086	0.234	3.500	0.050	60.	0.480	49143.
295	0.640	0.086	0.234	3.500	0.049	60.	0.480	52478.
194	0.895			3.497	0.099	45.	0.448	44194.
195	0.890			3.500	0.100	45.	0.445	43714.
196	0.885			3.500	0.100	45.	0.442	43429.
197	0.875			3.497	0.099	45.	0.438	44194.
198	0.885			3.496	0.100	45.	0.442	45767.
199	0.875			3.497	0.101	45.	0.438	44168.
200	0.890			3.500	0.101	45.	0.445	43281.
201	0.885			3.500	0.099	45.	0.442	45310.
222	0.635	0.084	0.234	3.500	0.099	60.	0.476	45310.
224	0.625	0.079	0.234	3.500	0.099	60.	0.469	47619.
31	0.656			3.496	0.254	60.	0.492	40879.
54	0.968			3.505	0.254	45.	0.484	40437.
55	0.937			3.497	0.253	45.	0.468	40916.
56	0.930			3.500	0.253	45.	0.465	39977.
123	0.890	0.211	0.234	3.500	0.252	45.	0.445	44218.
124	0.880	0.206	0.234	3.502	0.252	45.	0.440	44872.
125	0.880	0.206	0.234	3.500	0.253	45.	0.440	44043.
126	0.906	0.219	0.234	3.502	0.253	45.	0.453	41309.

curves. Figure 6 illustrates the probability curves computed for the data of Table VI when grouped according to specimen thickness. The shift of the probability curves to the right for the thinner specimens could be ascribed to a plane stress effect on residual strengths. However, the relatively low number of specimens at the thinner thicknesses and the overlapping of the curves at low probability levels precludes any strong conclusions in support of a large thickness effect on average strengths. For the range of thicknesses investigated, data from all thicknesses at a given nominal d_{im} were grouped together for the purpose of generating the probability curves of Fig. 4.

The manner of evaluation of the goodness-of-fit of the Weibull distribution to these data groupings via the Chi-squared test is described in the appendix. The correlation coefficient for each fit is given with the probability curves. Note that a 1.00 correlation indicates a perfect Weibull fit via a Chi-squared measure. Interpretation of the relatively low correlation numbers obtained for the current data is discussed in a later section.

5. Impact damaged specimens

As an example of the application of probability based fracture mechanics for impact penetration damage, the following statistical analysis was performed with residual strength data reported in the literature [8, 18, 19]. In these references residual strength tests were conducted upon high strength aluminum panels that were first subjected to

TABLE VI
Residual strengths 7075-T6 machined, controlled damage.

	Nominal $d_{im} = 0.630$				SHARP DAMAGE			
No	A	L	R	W	T	β	d_{im}	σ_c
250	0.630			3.500	0.047	90.	0.630	43161.
251	0.620			3.500	0.047	90.	0.620	42310.
252	0.620			3.500	0.047	90.	0.620	42310.
253	0.625			3.500	0.047	90.	0.625	42553.
254	0.615			3.500	0.047	90.	0.615	43465.
255	0.615			3.500	0.047	90.	0.615	41033.
256	0.620			3.500	0.047	90.	0.620	38298.
259	0.656			3.495	0.050	75.	0.612	53791.
260	0.650			3.500	0.051	75.	0.606	53109.
290	0.642	0.122	0.199	3.500	0.048	90.	0.642	38571.
181	0.615			3.502	0.099	90.	0.615	41823.
182	0.625			3.501	0.099	90.	0.625	40392.
183	0.635			3.500	0.099	90.	0.635	41847.
185	0.610			3.501	0.099	90.	0.610	41835.
186	0.620			3.501	0.099	90.	0.620	41547.
187	0.640			3.501	0.099	90.	0.640	39238.
220	0.620	0.111	0.199	3.500	0.101	90.	0.620	36492.
221	0.622	0.113	0.199	3.500	0.100	90.	0.622	36857.
11	0.650			3.496	0.255	90.	0.650	35334.
12	0.656			3.497	0.255	90.	0.656	35324.
13	0.629			3.504	0.254	90.	0.629	35730.
14	0.661			3.496	0.253	90.	0.661	36179.
15	0.650			3.497	0.253	90.	0.650	35943.
16	0.659			3.500	0.255	90.	0.659	34958.
17	0.670			3.503	0.252	90.	0.670	37383.
21	0.648			3.500	0.255	90.	0.648	34398.
22	0.664			3.501	0.255	90.	0.664	35620.
23	0.653			3.497	0.254	90.	0.653	37152.
24	0.647			3.500	0.255	90.	0.647	36303.
25	0.636			3.500	0.254	90.	0.636	35096.
26	0.655			3.500	0.254	90.	0.655	35658.
27	0.680			3.502	0.254	75.	0.634	39122.
29	0.667			3.496	0.253	75.	0.622	40362.
48	0.731			3.503	0.252	75.	0.682	37043.
49	0.695			3.503	0.254	75.	0.648	35740.
50	0.682			3.503	0.252	75.	0.636	38063.
51	0.812			3.504	0.253	60.	0.609	38578.
52	0.780			3.496	0.254	60.	0.585	39077.
53	0.785			3.500	0.254	60.	0.589	37120.
79	0.626	0.115	0.199	3.506	0.253	90.	0.626	36189.
80	0.629	0.116	0.199	3.504	0.254	90.	0.629	34831.
81	0.617	0.110	0.199	3.504	0.253	90.	0.617	35645.
82	0.655	0.117	0.211	3.502	0.252	75.	0.611	36034.
84	0.675	0.126	0.211	3.500	0.253	75.	0.630	35234.
85	0.690	0.134	0.211	3.506	0.252	75.	0.644	35314.
86	0.687	0.133	0.211	3.500	0.252	75.	0.641	35714.
87	0.715	0.147	0.211	3.498	0.252	75.	0.667	35735.
88	0.718	0.148	0.211	3.498	0.254	75.	0.670	35116.
89	0.665	0.122	0.211	3.497	0.253	75.	0.620	34586.
90	0.656	0.117	0.211	3.496	0.253	75.	0.612	36631.
119	0.796	0.179	0.219	3.500	0.253	60.	0.597	37267.

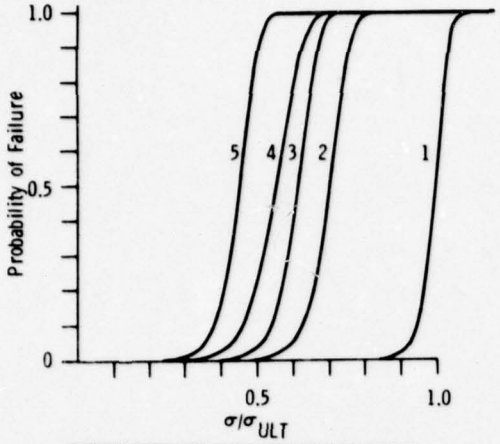

Curve	d_{im}	ν	η	Correlation
1	0.000	1.005	35.0	*
2	0.160	0.720	15.9	0.142
3	0.320	0.632	13.0	0.087
4	0.450	0.576	9.7	<0.01
5	0.630	0.469	10.7	<0.01

*Too few points for χ^2 correlation

Figure 4. Probability curves for high strength aluminum, machined, controlled damage specimens.

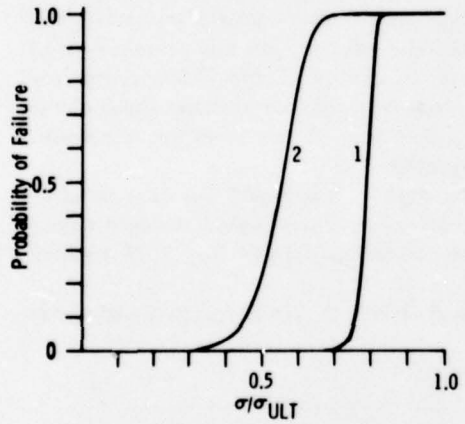

Curve	d_{im}	ν	η	Type Damage
1*	0.593	0.788	46.3	Smooth
2	0.450	0.576	9.7	Sharp

*Correlation <0.01

Figure 5. Influence of damage type on residual strength probability curves.

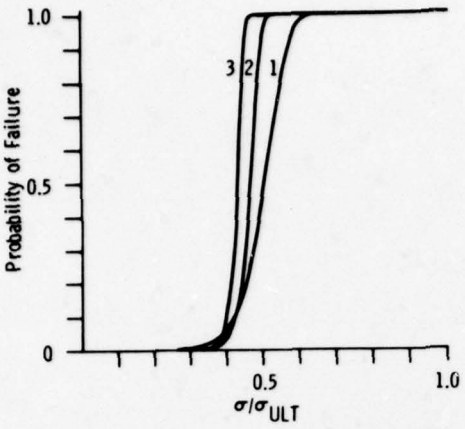

Curve	ν	η	Correlation	Thickness
1	0.523	9.90	*	0.050
2	0.472	19.23	*	0.100
3	0.432	29.03	<0.01	0.250
Table 6 - d_{im} = 0.630				
*Too few points for X^2 correlation				

Figure 6. Thickness effect on residual strength probability curves for machined, controlled damage specimens.

ballistic impact damage and then pulled to fracture in a uniaxial tensile test. The raw data from these tests were sorted and assembled into Table VII. Note that in this table the results were ordered by d_{im}. The data were originally obtained in a manner designed to study a spectrum of impact damage sizes over a range of materials and specimen thicknesses. For correlation with the Weibull function and comparison to the results of the machined, controlled damage specimens, Table VII is comprised only of data which was taken on aluminum specimens at thicknesses near those of the controlled damage tests. Also residual strength data was chosen from the references only in cases where d_{im} could be reliably computed.

Because of the spread in d_{im} values, the data was grouped for two nominal values, 1.70 and 2.60 inches, within ± 20% in each case. The residual strength values were normalized by an ultimate strength value consistent with the reported material properties.

Figure 7 presents the resulting probability of failure curves for impact damage in high strength aluminum.

6. Discussion of results

Figure 8 presents ν and η versus d_{im} for each set of residual strength data analyzed. It can serve to focus several key concepts that have evolved during this current work. First, again note that at no impact damage, $d_{im} = 0.0$, the values for ν and η are given for the machined aluminum specimens and the Freudenthal work on aircraft structural components. Then for the controlled machined damaged cracked specimens, the average strength values as reflected by ν fall as d_{im} is increased. The corresponding scatter of residual strengths is seen to rise somewhat as indicated by a drop in η over the same range of d_{im}. It is interesting to observe the measurable increase in ν for the

TABLE VII
Residual strengths impact damage.

A: 7075-T6 Aluminum, rolling grain transverse to loading axis
B: 7075-T6 Aluminum, rolling grain parallel to loading axis
C: 2024-T81 Aluminum, rolling grain transverse to loading axis
D: 2024-T3 Aluminum, rolling grain transverse to loading axis

Material	T (in)	W (in)	ρ^* (in)	β (°)	d_{im} (in)	σ_r (psi)	$\sigma_r/\sigma_{U.T}$	REF.
				Nominal $d_{im} = 1.70$ ($\pm 20\%$)				
C	0.160	12.	1.35	80.	1.31	41800.	0.624	[8]
A	0.032	12.	1.45	80.	1.41	41000.	0.539	[8]
B	0.250	12.	1.45	90.	1.45	60700.	0.720	[19]
B	0.500	12.	1.47	90.	1.47	56500.	0.670	[19]
A	0.032	12.	1.53	90.	1.53	37800.	0.497	[8]
A	0.250	12.	1.58	90.	1.58	49400.	0.648	[8]
B	0.500	12.	1.58	90.	1.58	64800.	0.760	[19]
A	0.500	7.	1.65	80.	1.60	45000.	0.592	[8]
B	0.250	12.	1.61	90.	1.61	49800.	0.590	[19]
B	0.125	12.	1.65	85.	1.64	58600.	0.773	[8]
B	0.500	8.	1.70	90.	1.70	60700.	0.720	[19]
B	0.190	18.	1.70	90.	1.70	41500.	0.546	[18]
A	0.250	12.	1.90	70.	1.68	35300.	0.465	[8]
A	0.500	7.	1.73	90.	1.73	51000.	0.671	[8]
B	0.500	12.	1.79	90.	1.79	58100.	0.690	[19]
B	0.500	12.	1.86	90.	1.86	51500.	0.610	[19]
B	0.250	12.	1.87	90.	1.87	53800.	0.630	[19]
D	0.250	12.	1.90	90.	1.90	45000.	0.692	[8]
A	0.250	12.	1.90	90.	1.90	37500.	0.493	[8]
B	0.250	12.	1.91	90.	1.91	62300.	0.730	[19]
B	0.500	12.	1.92	90.	1.92	47800.	0.560	[19]
B	0.500	12.	1.95	90.	1.95	41400.	0.490	[19]
				Nominal $d_{im} = 2.60$ ($\pm 20\%$)				
B	0.500	12.	2.14	90.	2.14	38500.	0.450	[19]
A	0.090	12.	2.16	90.	2.16	41200.	0.542	[8]
A	0.125	12.	2.30	90.	2.30	34000.	0.446	[8]
B	0.125	12.	2.35	90.	2.35	43300.	0.570	[8]
A	0.375	9.	2.40	90.	2.40	52000.	0.686	[8]
B	0.250	12.	2.42	90.	2.42	45400.	0.540	[19]
A	0.190	18.	2.96	64.	2.39	30700.	0.405	[18]
A	0.190	18.	2.96	66.	2.47	21500.	0.284	[18]
B	0.500	12.	2.56	90.	2.56	53600.	0.630	[19]
A	0.090	12.	2.70	90.	2.70	29400.	0.387	[8]
C	0.250	12.	2.75	85.	2.73	27500.	0.410	[8]
B	0.375	12.	2.99	75.	2.79	30500.	0.360	[19]
B	0.250	16.	2.82	90.	2.82	40100.	0.470	[19]
B	0.250	16.	2.85	90.	2.85	48200.	0.570	[19]
C	0.250	12.	3.22	80.	3.12	23400.	0.350	[8]
C	0.250	12.	3.25	80.	3.15	20400.	0.305	[8]

* When photograph of damage was not given in reference, tabulated LD for high angles of β was assumed to be reliable estimation of ρ.

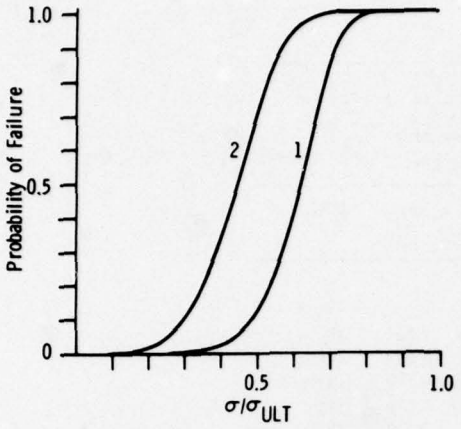

Curve	d_{im}	ν	η	Correlation
1	1.70	0.647	7.85	0.353
2	2.60	0.482	4.71	0.225

Figure 7. Probability curves for high strength aluminum, impact-damaged specimens.

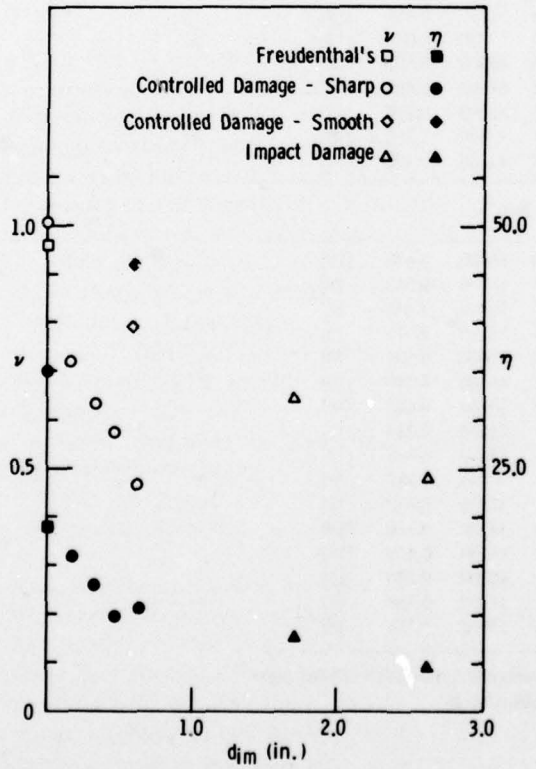

Figure 8. Weibull parameters *vs.* impact damage measure.

machined hole specimens over the cracked ones along with an η value, which was some five to ten times that for the cracked damage. Finally, note the apparent increase in average strengths for the impact damaged specimens over the trend in ν established by the controlled damage specimens. This was accompanied by a continued increase in scatter as indicated by the further decline in η values. After consideration of photographs of the impact damaged specimens reported in Ref. [19], it was concluded that both the increase in scatter and apparent rise in the average strength of the impact damage results were due in part to the nature of the damage detail. For example, for many of the thicker specimens, the high velocity projectiles used to penetrate the panels often created damage which consisted primarily of a through hole plus an extended spall surface on the exit side. Little evidence of extensive radial crack formation was indicated. Therefore, those specimens acted more like the smooth damage of the controlled damage tests and caused an apparent increase in the average residual strength. This fact may also account for an apparent reversal of the plane stress toughness effect for impact residual strengths as reported in the literature [20].

The residual strengths for the smooth damage specimens had the least scatter as measured by η of any of the test groups. It was better than the standard tensile test results by approximately 30%. This implies that the stress concentration in the smooth hole specimens strongly focused the conditions for failure such that the variation in resulting residual strengths was less than that inherent for failure under gross necking as associated with the uniaxial tension test. Also, the specimen thickness appears to have had a minimal influence in the scatter of the smooth damage data. In contrast the variability of the sharp machined damage residual strengths is measurably higher as indicated by their lower η values. This could reflect the sensitive nature of the mechanism of crack tip extension to local crack tip geometry and specimen thickness. In fact, Fig. 6 shows that in the case of the constant thickness, 0.250 inch, specimens with crack damage, $d_{im} = 0.630$, a Weibull analysis on thirty-three specimens resulted in a significantly reduced scatter in residual strengths over the entire group of Table VI which included all three thicknesses at a $d_{im} = 0.630$; $\eta = 29.03$ versus 10.7. These points become important when interpreting impact damage results where a mixture of smooth and sharp damage detail produces higher average strengths, similar to smooth damage data, but significantly lower η values, typical to the variability influences associated with sharp damage data.

Whereas ν and η reflect the average strength and scatter respectively for a given data set, the Chi-squared correlation number reflects the degree to which the Weibull density function's shape corresponds to that of the histogram of experimental cumulative probabilities. The following appendix reveals in detail that for the data under current consideration, two separate cases arise with respect to the low correlation numbers. For the case of the machined, controlled damage specimens, the low correlation number is due to the non-random nature of each test data sample as a result of the sub set groupings at different but specified thicknesses. However, the low correlation number has little practical significance because the resulting probability curves of Figs. 4 to 6 are each the integral of a density function which has its maximum influence over a small interval of the z domain. It is therefore insensitive to the exact shape of the density function and depends more upon the average strength and scatter parameters.

For the case of impact damage, the statistical scatter extends over a much greater portion of the z domain, and the correlation number becomes more important in reflecting possible significant error in the resulting probability curves. The correlation numbers of Fig. 7 for the impact damage probability curves are seen to be sig-

nificantly improved over the controlled damage case. In fact, given that the number of impact damage specimens available for statistical analysis was near the minimum allowable for a meaningful Chi-squared test, the resulting correlation numbers are perhaps as good as can be expected.

These results point to the need for careful consideration of the following guidelines for the future application of a probability based fracture mechanics approach to impact penetration damage.

i. Isolate and group specimens according to material, thickness, and d_{im} in order to derive the most reliable statistics as measured by a maximum possible η value and a maximum Chi-squared correlation.

ii. Test with enough replications at each grouping to ensure a meaningful correlation via a Chi-squared test. A minimum number of replications appears to be twenty to thirty; a better number would be near fifty.

Because of the cost factor associated with these recommendations, future research into the development of simulation techniques via numerical computer to obtain probability of failure curves for impact damage would appear to offer a potential alternative to minimize expense.

7. Conclusions

This work represents the first step in the development of a statistical approach for evaluating the residual strength of impact penetration damaged structures. It establishes a philosophy and accompanying methodology for the assessment of the degree of damage resulting from an impact penetration along with corresponding evaluation of the residual strength in terms of a probability of failure. This is in contrast to previous fail/no fail deterministic approaches which are unable to account for large scatter in the residual strength data taken from impact-damaged specimens. As such, the statistical approach is of immediate use to the engineering community in beginning to include quantitative probability based fracture mechanics in early phases of design for impact penetration damage. As a larger data base is collected following the guidelines recommended in this paper, precise calculations of the probability of failure for impact-damaged structures will be possible beyond the estimations now attainable for the limited damage range of Figs. 7 and 8.

Recognizing that the formulation and parameters presented in this paper are strictly for the case of uniaxial stress states, future research will be involved in generalizing the statistical approach for multiaxial stress fields. Note that past workers [8] have attempted to extend uniaxial test data by characterizing the stress field remote from the damage in terms of the largest principal stress. While such an approach could be used with the probability functions as provided in this paper, it is recommended only in cases where one stress component obviously dominates the stress field in the vicinity of the damage.

For more general states of multiaxial stress, two avenues of research must be explored. One consists of seeking ways to combine the uniaxial probabilities to form a practical estimation of the probability of failure for an impact penetration damage in a multiaxial stress field. The second involves the development of a multiaxial version of d_{im} with associated probability correlations. For example, following the manner of derivation of d_{im} given in this paper, but where the inclined crack is situated in a multiaxial stress field, σ_1 and σ_2, a relationship between the fracture stresses and the damage parameters, ρ and β, becomes

$$C_0^2 = \sigma_1^2(\pi\rho/2)[\sin^2\beta + (\sigma_2/\sigma_1)^2\cos^2\beta + 4(\sigma_2/\sigma_1)\sin^2\beta\cos^2\beta] \tag{14}$$

where β is measured from the direction of σ_1.

This expression illustrates that the damage factor is not a simple function of ρ and β as in the uniaxial case, but contains the ratio of the multiaxial stress components as well. More work is obviously required to evaluate this and alternative precise measures of impact damage in a multiaxial stress field.

Finally, recall that the Weibull two-parameter probability function was utilized in this current effort based upon the earlier work by Freudenthal, who identified it as the best function to use in the statistical representative of residual strengths of undamaged structural components. It is important to note, however, that the probability based fracture mechanics approach is not limited to any one density function. Future work should explore the utilization of other density functions to represent the scatter of residual strengths of impact-damaged components with comparisons based upon the four factors for goodness of fit assessment outlined in the appendix of this paper.

Appendix

The Chi-squared test for goodness of fit provides a means for estimating how closely a given Weibull function matches the distribution of residual strength data from which it was derived. Figure 9 illustrates the distribution of residual strengths in the form of a histogram for the test data of Tables II and III where $d_{im} = 0.593$ and 0.160 inch, respectively. Superimposed upon each figure is the corresponding Weibull probability density function. The ordinate scale has been chosen such that the total area under the density function is unity and the histogram was constructed such that the area which it encloses is also equal to unity.

A key step in establishing a correlation number by the Chi-squared test is the division of the probability density area into known probabilities; it is convenient to make these sub-areas equal. The intervals on the z axis which establish the boun-

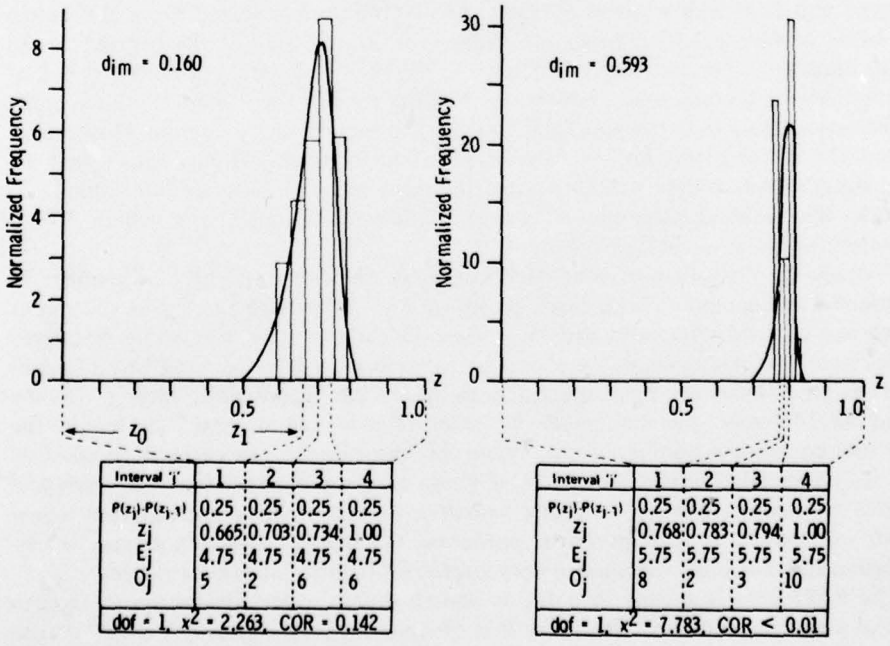

Interval 'j'	1	2	3	4
$P(z_j)-P(z_{j-1})$	0.25	0.25	0.25	0.25
z_j	0.665	0.703	0.734	1.00
E_j	4.75	4.75	4.75	4.75
O_j	5	2	6	6

dof = 1, x^2 = 2.263, COR = 0.142

Interval 'j'	1	2	3	4
$P(z_j)-P(z_{j-1})$	0.25	0.25	0.25	0.25
z_j	0.768	0.783	0.794	1.00
E_j	5.75	5.75	5.75	5.75
O_j	8	2	3	10

dof = 1, x^2 = 7.783, COR < 0.01

Figure 9. Chi-squared correlation for Weibull fits.

daries of the sub-areas are determined from the inversion of the Eqn. (7).

$$z_j = \nu[-\ln(1 - P(z_j))]^{1/\eta} \tag{A1}$$

where $P(z_j)$ is the cumulative probability up to and including interval, j.

Comparison is then made between the number of observed test values which lie in each sub-area and those that would be expected based upon the sub-area probability and the total number of test strength values in the sample. This comparison is made through the Chi-squared parameter defined by

$$\chi^2 = \sum_{j=1}^{N} (O_j - E_j)^2 / E_j \tag{A2}$$

where

E_j = expected number in interval, j
O_j = observed number in interval, j
N = total number of sub-area intervals

Based upon the Chi-squared value and the number of independent sub-area intervals, tables are available [21] which indicate the degree of correlation between the Weibull distribution and the actual residual strength distribution. The number of independent sub-areas are termed the degrees of freedom and for the two-parameter Weibull fit is given by

$$dof = N - 3 \tag{A3}$$

where the constant, 3, accounts for the dependent relationship between the experimental data and the two Weibull parameters along with the constraint that all the sub-area probabilities must add to unity.

From consideration of Fig. 9, four factors emerge as equally important in assessing how well a given Weibull fit corresponds to a distribution of residual strengths and how well a given Weibull density function may represent the actual probability of failure curve. First, the shape and relative size of the histogram and density function, when both are normalized to the same total area, provide a check of the suitability of the assumed distribution. For the case of the 0.160 data the Weibull distribution appears to correspond quite well to the normalized histogram. However, a detailed plot of the histogram and Weibull function for the 0.593 data shows that the actual strength data reflect a bi-modal distribution which can be traced to a thickness effect in the residual strengths of panels with smooth holes and which is not accounted for by a Weibull distribution.

Second, the Chi-squared value itself is greatly influenced by the total number of specimens. For example in both cases shown on Fig. 9, the total number of specimens in each set was such that the expected value in each interval was some fractional number near five. Thus, since the observed value in each interval must be an integer near five, an error arises from the fractions which can significantly alter χ^2. In the case of the 0.160 data, this along with the larger difference in interval 2 has lead to the rather low correlation number, 0.142. While this third factor, the correlation number, itself, is an important number in strictly defining a correspondence between statistical fit and experimental data, it is highly sensitive to inaccuracies arising from a low number of specimens. For practical purposes, the density function having a low correlation number may yet yield a very useful probability of failure curve.

The 0.593 data is a case in point as shown in Fig. 9 and illustrates the fourth factor in assessing statistical fits. Here it is obvious that the detailed bi-modal nature of the data cannot be closely fit by the Weibull distribution, and a very low

correlation number results. However, because the distribution is very narrow, the bi-modal nature of the sample is a higher-order effect with respect to the resulting shape and location of the probability of failure curve. The Weibull function for that data set accurately reflects both the average strength and scatter band. It leads to a probability of failure curve which is quite accurate and useful for practical purposes even though the correlation number is low. Therefore, assessment of the effect of the width of the data's scatter band upon the computational accuracy of the probability curve is an important factor in evaluating the need for a close, detailed matching of the experimental histogram and the derived Weibull density function.

In conclusion, all four factors become important in assessing the degree of success in representing the statistical nature of a given set of test data. In order to optimize the goodness-of-fit by all four factors in future extensions of the statistical approach, the guidelines presented in the discussion section of this paper are recommended.

REFERENCES

[1] M.J. Rich, "Vulnerability Considerations in the Design of Rotary Wing Aircraft Structures", *Proceedings of the Air Force Conference on Fatigue and Fracture of Aircraft Structures and Materials*, AFFDL TR 70-144 (Dec. 1969) 635–651.

[2] R.C. Combes, *Journal of Aircraft*, 7 (Jan.–Feb. 1970) 18–20.

[3] W.J. Shuler and D.S. Morcock, *Journal of Aircraft*, 6 (Sept.–Oct. 1969) 416–424.

[4] M.D. Campbell, J.F. Haskins and J.E. Jensen, "Correlation of Residual Strength of Ballistically Damaged Panels with Fracture Toughness Theory", *Proceedings of the Air Force Conference on Fatigue and Fracture of Aircraft Structures and Materials*, AFFDL TR 70-144 (Dec. 1969) 539–555.

[5] J.F. Lundeberg, P.H. Stern, and R.J. Bristow, "Meteoroid Protection for Spacecraft Structures", NASA CR-54201 (Oct. 1965).

[6] G.D. Fearnehough, D.W. Jude, and R.T. Weiner, "The Arrest of Brittle Fracture in Pipelines", *Practical Application of Fracture Mechanics to Pressure Vessel Technology*, The Institution of Mechanical Engineers, London (1971) 156–162.

[7] T.P. Rich, "Three Approaches for Estimation of Residual Strengths of Ballistically Damaged Materials", *Proceedings of the Army Symposium on Solid Mechanics, 1972, The Role of Mechanics in Design Ballistic Problems*, AMMRC MS 73-2 (Sept. 1973) 483–492.

[8] G.T. Burch and J.G. Avery, "An Aircraft Structural Combat Damage Model", Vols. I, II, III, and Design Handbook, Technical Reports AFFDL TR 50–115, Wright-Patterson Air Force Base, Ohio (Nov. 1970).

[9] J.G. Avery, *Engineering Fracture Mechanics*, 4 (1972) 749–763.

[10] P.C. Paris and G.C. Sih, "Stress Analysis of Cracks", *Fracture Toughness Testing and Its Applications*, American Society for Testing and Materials, STP 381 (1965) 67.

[11] G.C. Sih, *International Journal of Fracture*, 10 (Sept. 1974) 319.

[12] T.P. Rich, "Evaluation of Current Fracture Criteria", currently under preparation.

[13] A.M. Freudenthal and P.Y. Wang, *Journal of Aircraft*, 7 (May–June 1970) 205–210.

[14] W. Weibull, *Journal of Applied Mechanics* (Sept. 1951) 293–297.

[15] J.R. King, "Graphical Data Analysis with Probability Papers", published by TEAM, Special Purpose Graph Papers, Lowell, Massachusetts (1969).

[16] I. Bazovsky, *Reliability Theory and Practice*, Prentice-Hall Space Technology Series, Prentice-Hall Inc., Englewood Cliffs, New Jersey (1961).

[17] J. Adachi, Mechanics Research Laboratory, Army Materials and Mechanics Research Center, Watertown, Massachusetts, private communication.

[18] R.G. Forman, W.H. Parker, A.W. Gunderson, and A. Bilek, "Vulnerability of Aircraft Structures Exposed to Small Arms Fire Projectile Impact Damage", Technical Report AFFDL TR 67-157, Wright–Patterson Air Force Base, Ohio (Feb. 1968).

[19] J.E. Jensen, P. Thorndyke, and M. Campbell, "Aircraft Wing Structural Concepts with Improved Ballistic Damage Tolerance", GDC-DDG 69-002, Vol. II, General Dynamics/Convair Division (Oct. 1969).

[20] J.E. Jensen, "The Ballistic Damage Characteristics and Damage Tolerance of Wing Structural Elements", *Damage Tolerance in Aircraft Structures*, ASTM STP 486, American Society for Testing and Materials (1971) 215–229.

[21] P.G. Hoel, *Introduction to Mathematical Statistics*, John Wiley and Sons, Inc., New York (1971).

RÉSUMÉ

Le mémoire présente une nouvelle méthode pour vérifier la résistance résiduelle de composants structuraux ayant subi un dommage suite à un impact pénétrant. La méthode est basée sur l'application de la fonction de densité de probabilité de Weibull, pour tenir compte de la dispersion appréciable de résistances résiduelles, qui découle de la nature statistique du dommage par impact (fissure, trous et écaillages en surface).

Pour mesurer l'étendue d'une configuration d'un dommage par impact, on présente un nouveau paramètre basé sur la solution applicable à une fissure inclinée dans un champ de tension uniaxial, et basé sur un critère de rupture obtenu par voie expérimentale, pour des configurations de fissure de mode mixte.

Les résultats des essais sont présentés pour des résistances résiduelles d'éprouvettes endommagées et usinées afin de vérifier la nature statistique qui caractérise un détail d'endommagement extérieur, un trou à paroi lisse et une fissure aigüe. Enfin, des courbes de probabilité de rupture sont fournies pour des panneaux d'aluminium 7075-TG soumis à tension uniaxiale et comportant à la fois un endommagement par usinage et par impact.

DISTRIBUTION LIST

No. of Copies	To
1	Office of the Director, Defense Research and Engineering, The Pentagon, Washington, D.C. 20301
12	Commander, Defense Documentation Center, Cameron Station, Building 5, 5010 Duke Street, Alexandria, Virginia 22314
1	Metals and Ceramics Information Center, Battelle Columbus Laboratories, 505 King Avenue, Columbus, Ohio 43201
	Deputy Chief of Staff, Research, Development, and Acquisition, Headquarters Department of the Army, Washington, D. C. 20310
1	ATTN: DAMA-ARZ
	Commander, Army Research Office, P. O. Box 12211, Research Triangle Park, North Carolina 27709
1	ATTN: Information Processing Office
1	Dr. F. W. Schmiedeshoff
	Commander, U. S. Army Materiel Development and Readiness Command, 5001 Eisenhower Avenue, Alexandria, Virginia 22333
1	ATTN: DRCLDC, Mr. R. Zentner
	Commander, U. S. Army Communications Research and Development Command, Fort Monmouth, New Jersey 07703
1	ATTN: DRCDO-GG-TD
1	DRCDO-GG-DM
1	DRCDO-GG-E
1	DRCDO-GG-EA
1	DRCDO-GG-ES
1	DRCDO-GG-EG
1	DRCDO-GG-EI
	Commander, U. S. Army Missile Research and Development Command, Redstone Arsenal, Alabama 35809
1	ATTN: DRDMI-RKK, Mr. C. Martens, Bldg. 7120
	Commander, U. S. Army Natick Research and Development Command, Natick, Massachusetts 01760
1	ATTN: Technical Library
1	Dr. E. W. Ross
1	DRDNA-UE, Dr. L. A. McClaine
	Commander, U. S. Army Satellite Communications Agency, Fort Monmouth, New Jersey 07703
1	ATTN: Technical Document Center
	Commander, U. S. Army Tank-Automotive Research and Development Command, Warren, Michigan 48090
1	ATTN: DRDTA-RKA
1	DRDTA-UL, Technical Library
	Commander, U. S. Army Armament Research and Development Command, Dover, New Jersey 07801
2	ATTN: Technical Library
1	DRDAR-SCM, J. D. Corrie
1	Dr. J. Fraiser
	Commander, White Sands Missile Range, New Mexico 88002
1	ATTN: STEWS-WS-VT
	Commander, Aberdeen Proving Ground, Maryland 21005
1	ATTN: STEAP-TL, Bldg. 305
	Commander, Frankford Arsenal, Philadelphia, Pennsylvania 19137
1	ATTN: Library, H1300, Bldg. 51-2
	Commander, U. S. Army Armament Research and Development Command, Aberdeen Proving Ground, Maryland 21010
1	ATTN: DRDAR-QAC-E
	Commander, U. S. Army Ballistic Research Laboratory, Aberdeen Proving Ground, Maryland 21005
1	ATTN: Dr. R. Vitali
1	Dr. G. L. Filbey
1	Dr. W. Gillich
1	Mr. A. Elder
1	DRDAR-TSB-S (STINFO)
	Commander, Harry Diamond Laboratories, 2800 Powder Mill Road, Adelphi, Maryland 20783
1	ATTN: Technical Information Office
	Commander, Picatinny Arsenal, Dover, New Jersey 07801
1	ATTN: Mr. A. M. Anzalone, Bldg. 3401
1	Mr. J. Pearson
1	G. Randers-Pehrson
1	Mr. A. Garcia
1	SARPA-RT-S
	Commander, Redstone Scientific Information Center, U. S. Army Missile Research and Development Command, Redstone Arsenal, Alabama 35809
1	ATTN: DRDMI-TB
	Commander, Watervliet Arsenal, Watervliet, New York 12189
1	ATTN: Dr. T. Davidson
1	Mr. D. P. Kendall
1	Mr. J. F. Throop
	Commander, U. S. Army Foreign Science and Technology Center, 220 7th Street, N. E., Charlottesville, Virginia 22901
1	ATTN: Mr. Marley, Military Tech
	Chief, Benet Weapons Laboratory, LCWSL, USA ARRADCOM, Watervliet Arsenal, Watervliet, New York 12189
1	ATTN: DRDAR-LCB-TL
	Director, Eustis Directorate, U. S. Army Air Mobility Research and Development Laboratory, Fort Eustis, Virginia 23604
1	ATTN: Mr. J. Robinson, DAVDL-E-MOS (AVRADCOM)
	U. S. Army Aviation Training Library, Fort Rucker, Alabama 36360
1	ATTN: Building 5906-5907
	Commander, U. S. Army Agency for Aviation Safety, Fort Rucker, Alabama 36362
1	ATTN: Librarian, Bldg. 4905
	Commander, USACDC Air Defense Agency, Fort Bliss, Texas 79916
1	ATTN: Technical Library
	Commander, U. S. Army Engineer School, Fort Belvoir, Virginia 22060
1	ATTN: Library
	Commander, U. S. Army Engineer Waterways Experiment Station, Vicksburg, Mississippi 39180
1	ATTN: Research Center Library
	Commander, U. S. Army Mobility Equipment Research and Development Center, Fort Belvoir, Virginia 22060
1	ATTN: DRDME-MW, Dr. J. W. Bond
	Commander, Naval Air Engineering Center, Lakehurst, New Jersey 08733
1	ATTN: Technical Library, Code 1115
	Director, Structural Mechanics Research, Office of Naval Research, 800 North Quincy Street, Arlington, Virginia 22203
1	ATTN: Dr. N. Perrone
	Naval Air Development Center, Aero Materials Department, Warminster, Pennsylvania 18974
1	ATTN: J. Viglione
	David Taylor Naval Ship Research and Development Laboratory, Annapolis, Maryland 21402
1	ATTN: Dr. H. P. Chu
	Naval Research Laboratory, Washington, D.C. 20375
1	ATTN: C. D. Beachem, Head, Adv. Mat'ls Tech Br. (Code 6310)
1	Dr. J. M. Krafft - Code 8430
1	E. A. Lange
1	Dr. P. P. Puzak
1	R. J. Sanford - Code 8436
1	A. M. Sullivan
1	R. W. Rice
1	S. W. Freiman
	Chief of Naval Research, Arlington, Virginia 22217
1	ATTN: Code 471
	Naval Weapons Laboratory, Washington, D.C. 20390
1	ATTN: H. W. Romine, Mail Stop 103
1	Ship Research Committee, Maritime Transportation Research Board, National Research Council, 2101 Constitution Avenue, N. W., Washington, D.C. 20418
	Air Force Materials Laboratory, Wright-Patterson Air Force Base, Ohio 45433
2	ATTN: AFML (MXE), E. Morrissey
1	AFML (LC)
1	AFML (LLP), D. M. Forney, Jr.
1	AFML (LNC), T. J. Reinhart
1	AFML (MBC), Mr. Stanley Schulman
1	AFFDL (FB), Dr. J. C. Halpin

No. of Copies	To
	Air Force Flight Dynamics Laboratory, Wright-Patterson Air Force Base, Ohio 45433
1	ATTN: AFFDL (FBS), C. Wallace
1	AFFDL (FBE), G. D. Sendeckyj
	National Aeronautics and Space Administration, Washington, D.C. 20546
1	ATTN: Mr. B. G. Achhammer
1	Mr. G. C. Deutsch - Code RW
	National Aeronautics and Space Administration, Marshall Space Flight Center, Huntsville, Alabama 35812
1	ATTN: R. J. Schwinghamer, EH01, Dir., M&P Lab
1	Mr. W. A. Wilson, EH41, Bldg. 4612
	National Aeronautics and Space Administration, Langley Research Center, Hampton, Virginia 23665
1	ATTN: Mr. H. F. Hardrath, Mail Stop 188M
1	Mr. R. Foye, Mail Stop 188A
	National Aeronautics and Space Administration, Lewis Research Center, 21000 Brookpark Road, Cleveland, Ohio 44135
1	ATTN: Mr. S. S. Manson
1	Dr. J. E. Srawley, Mail Stop 105-1
1	Mr. W. F. Brown, Jr.
1	Mr. R. F. Lark, Mail Stop 49-3
1	Mr. M. H. Hirschberg, Head, Fatigue Research Section, Mail Stop 49-1
	Lockheed-Georgia Company, 86 South Cobb Drive, Marietta, Georgia 30063
1	ATTN: Materials & Processes Eng. Dept. 71-11, Zone 54
	National Bureau of Standards, U. S. Department of Commerce, Washington, D.C. 20234
1	ATTN: Mr. J. A. Bennett
1	Mechanical Properties Data Center, Belfour Stulen Inc., 13917 W. Bay Shore Drive, Traverse City, Michigan 49684
1	Mr. W. F. Anderson, Atomics International, Canoga Park, California 91303
	Midwest Research Institute, 425 Coker Boulevard, Kansas City, Missouri 64110
1	ATTN: Mr. C. Q. Bowles
1	Mr. G. Gross
1	Dr. J. Charles Grosskreutz, Asst. Dir. for Research, Solar Energy Research Institute, 1536 Cole Boulevard, Golden, Colorado 80401
1	Mr. A. Hurlich, Convair Div., General Dynamics Corp., Mail Zone 630-01, P. O. Box 80847, San Diego, California 92138
	Southwest Research Institute, 8500 Culebra Road, San Antonio, Texas 78284
1	ATTN: Dr. P. Francis
1	Dr. W. Baker
1	Mr. J. G. Kaufman, Alcoa Research Laboratories, New Kensington, Pennsylvania 15068
1	Mr. P. N. Randall, TRW Systems Group - 0-1/2210, One Space Park, Redondo Beach, California 90278
1	Dr. E. A. Steigerwald, TRW Metals Division, P. O. Box 250, Minerva, Ohio 44657
1	Dr. George R. Irwin, Department of Mechanical Engineering, University of Maryland, College Park, Maryland 20742
1	Mr. W. A. Van der Sluys, Research Center, Babcock and Wilcox, Alliance, Ohio 44601
1	Mr. B. M. Wundt, 2346 Shirl Lane, Schenectady, New York 12309

No. of Copies	To
	Battelle Columbus Laboratories, 505 King Avenue, Columbus, Ohio 43201
1	ATTN: Mr. J. Campbell
1	Dr. G. T. Hahn
1	R. G. Hoagland, Metal Science Group
1	Dr. E. Rybicki
	General Electric Company, Schenectady, New York 12010
1	ATTN: Mr. A. J. Brothers, Materials & Processes Laboratory
	General Electric Company, Schenectady, New York 12309
1	ATTN: Mr. H. F. Bueckner, Large Steam Turbine Generator Department
1	Mr. S. Yukawa, Metallurgy Unit
1	Mr. E. E. Zwicky, Jr.
	General Electric Company, Knolls Atomic Power Laboratory, P. O. Box 1072, Schenectady, New York 12301
1	ATTN: Mr. F. J. Mehringer
1	Dr. L. F. Coffin, Room 1C41-K1, Corp. R&D, General Electric Company, P. O. Box 8, Schenectady, New York 12301
	United States Steel Corporation, Monroeville, Pennsylvania 15146
1	ATTN: Mr. S. R. Novak
1	Dr. A. K. Shoemaker, Research Laboratory, Mail Stop 78
	Westinghouse Electric Company, Bettis Atomic Power Laboratory, P. O. Box 109, West Mifflin, Pennsylvania 15122
1	ATTN: Mr. M. L. Parrish
	Westinghouse Research and Development Center, 1310 Beulah Road, Pittsburgh, Pennsylvania 15235
1	ATTN: Mr. E. T. Wessel
1	Mr. M. J. Manjoine
1	Dr. Alan S. Tetelman, Failure Analysis Associates, Suite 4, 11777 Mississippi Ave., Los Angeles, California 90025
	Brown University, Providence, Rhode Island 02912
1	ATTN: Prof. J. R. Rice
1	Prof. W. N. Findley, Division of Engineering, Box D
1	Prof. P. C. Paris
	Carnegie-Mellon University, Department of Mechanical Engineering, Schenley Park, Pittsburgh, Pennsylvania 15213
1	ATTN: Dr. J. L. Swedlow
1	Prof. J. D. Lubahn, Colorado School of Mines, Golden, Colorado 80401
1	Prof. J. Dvorak, Civil Engineering Department, Duke University, Durham, North Carolina 27706
	George Washington University, School of Engineering and Applied Sciences, Washington, D.C. 20052
1	ATTN: Dr. H. Liebowitz
	Lehigh University, Bethlehem, Pennsylvania 18015
1	ATTN: Prof. G. C. Sih
1	Prof. R. Roberts
1	Prof. R. P. Wei
1	Prof. F. Erodgan
	Terra Tek, University Research Park, 420 Wakara Way, Salt Lake City, Utah 84108
1	ATTN: Dr. A. Jones
	P. R. Mallory Company, Inc., 3029 East Washington Street, Indianapolis, Indiana 46206
1	ATTN: Technical Library
1	Librarian, Material Sciences Corporation, Blue Bell Office Campus, Merion Towle House, Blue Bell, Pennsylvania 19422

No. of Copies	To
	Massachusetts Institute of Technology, Cambridge, Massachusetts 02139
1	ATTN: Prof. B. L. Averbach, Materials Center, 13-5082
1	Prof. F. A. McClintock, Room 1-304
1	Prof. R. M. Pelloux
1	Prof. T. H. H. Pian, Department of Aeronautics and Astronautics
1	Prof. A. S. Argon, Room 1-306
1	Prof. J. N. Rossettos, Department of Mechanical Engineering, Northeastern University, Boston Massachusetts 02115
1	Prof. R. Greif, Department of Mechanical Engineering, Tufts University, Medford, Massachusetts 02155
1	Dr. D. E. Johnson, AVCO Systems Division, Wilmington, Massachusetts 01887
	University of Delaware, Department of Aerospace and Mechanical Engineering, Newark, Delaware 19711
1	ATTN: Prof. B. Pipes
1	Prof. J. Vinson
	Syracuse University, Department of Chemical Engineering and Metallurgy, 409 Link Hall, Syracuse, New York 13210
1	ATTN: Mr. H. W. Liu
1	Dr. V. Weiss, Metallurgical Research Labs., Bldg. D-6
1	Prof. E. R. Parker, Department of Materials Science and Engineering, University of California, Berkeley, California 94700
1	Prof. W. Goldsmith, Department of Mechanical Engineering, University of California, Berkeley, California 94720
	University of California, Los Alamos Scientific Laboratory, Los Alamos, New Mexico 87544
1	ATTN: Dr. R. Karpp
1	Prof. A. J. McEvily, Metallurgy Department U-136, University of Connecticut, Storrs, Connecticut 06268

No. of Copies	To
1	Prof. D. Drucker, Dean of School of Engineering, University of Illinois, Champaign, Illinois 61820
	University of Illinois, Urbana, Illinois 61801
1	ATTN: Prof. H. T. Corten, Department of Theoretical and Applied Mechanics, 212 Talbot Laboratory
1	Prof. T. J. Dolan, Department of Theoretical and Applied Mechanics
1	Prof. J. Morrow, 321 Talbot Laboratory
1	Mr. G. M. Sinclair, Department of Theoretical and Applied Mechanics
1	Dr. T. Lardner, Department of Theoretical and Applied Mechanics
1	Prof. R. I. Stephens, Materials Engineering Division, University of Iowa, Iowa City, Iowa 52242
1	Prof. D. K. Felbeck, Department of Mechanical Engineering, University of Michigan, 2046 East Engineering, Ann Arbor, Michigan 48109
1	Dr. M. L. Williams, Dean of Engineering, 240 Benedum Hall, University of Pittsburgh, Pittsburgh, Pennsylvania 15260
1	Prof. A. Kobayashi, Department of Mechanical Engineering, FU-10, University of Washington, Seattle, Washington 98195
	State University of New York at Stony Brook, Stony Brook, New York 11790
1	ATTN: Prof. Fu-Pen Chiang, Department of Mechanics
	Denver Research Institute, 2390 South University Boulevard, Denver, Colorado 80210
1	ATTN: Dr. R. Recht
	Director, Army Materials and Mechanics Research Center, Watertown, Massachusetts 02172
2	ATTN: DRXMR-PL
1	DRXMR-AG-MD
7	Authors

Army Materials and Mechanics Research Center,
Watertown, Massachusetts 02172
PROBABILITY BASED FRACTURE MECHANICS FOR IMPACT PENETRATION DAMAGE - Thomas P. Rich, Peter G. Tracy, Louis R. Tramontozzi, Jiro Adachi, Milo Benicek, Alan H. Katz, and Wilbert J. Foster

AD____________

UNCLASSIFIED
UNLIMITED DISTRIBUTION

Key Words

Fracture
Probability
Impact

Technical Report AMMRC TR 78-24, June 1978, 24 pp - illus-tables, D/A Project 1L162105AH84
AMCMS Code 612105.H840011

This paper presents a new method for assessing the residual strength of structural components which have sustained impact penetration damage. The method is based upon the application of the Weibull probability density function to account for the significant scatter in residual strengths which result from the random nature of impact damage detail (cracks, holes, and spall surfaces). To measure the extent of an impact damage pattern, a new parameter is presented which is based upon the solution for an inclined crack in a uniaxial tension field and an experimentally obtained fracture criterion for mixed mode crack configurations. Test results are presented for residual strengths of machined damage specimens to ascertain the statistical nature which arises from extreme damage detail, smooth holes and sharp cracks. Finally, probability of failure curves are given for both machined (7075-T6) and impact damage (7075-T6 and 2024-T81) in aluminum uniaxial tension panels.

Army Materials and Mechanics Research Center,
Watertown, Massachusetts 02172
PROBABILITY BASED FRACTURE MECHANICS FOR IMPACT PENETRATION DAMAGE - Thomas P. Rich, Peter G. Tracy, Louis R. Tramontozzi, Jiro Adachi, Milo Benicek, Alan H. Katz, and Wilbert J. Foster

AD____________

UNCLASSIFIED
UNLIMITED DISTRIBUTION

Key Words

Fracture
Probability
Impact

Technical Report AMMRC TR 78-24, June 1978, 24 pp - illus-tables, D/A Project 1L162105AH84
AMCMS Code 612105.H840011

This paper presents a new method for assessing the residual strength of structural components which have sustained impact penetration damage. The method is based upon the application of the Weibull probability density function to account for the significant scatter in residual strengths which result from the random nature of impact damage detail (cracks, holes, and spall surfaces). To measure the extent of an impact damage pattern, a new parameter is presented which is based upon the solution for an inclined crack in a uniaxial tension field and an experimentally obtained fracture criterion for mixed mode crack configurations. Test results are presented for residual strengths of machined damage specimens to ascertain the statistical nature which arises from extreme damage detail, smooth holes and sharp cracks. Finally, probability of failure curves are given for both machined (7075-T6) and impact damage (7075-T6 and 2024-T81) in aluminum uniaxial tension panels.

Army Materials and Mechanics Research Center,
Watertown, Massachusetts 02172
PROBABILITY BASED FRACTURE MECHANICS FOR IMPACT PENETRATION DAMAGE - Thomas P. Rich, Peter G. Tracy, Louis R. Tramontozzi, Jiro Adachi, Milo Benicek, Alan H. Katz, and Wilbert J. Foster

AD____________

UNCLASSIFIED
UNLIMITED DISTRIBUTION

Key Words

Fracture
Probability
Impact

Technical Report AMMRC TR 78-24, June 1978, 24 pp - illus-tables, D/A Project 1L162105AH84
AMCMS Code 612105.H840011

This paper presents a new method for assessing the residual strength of structural components which have sustained impact penetration damage. The method is based upon the application of the Weibull probability density function to account for the significant scatter in residual strengths which result from the random nature of impact damage detail (cracks, holes, and spall surfaces). To measure the extent of an impact damage pattern, a new parameter is presented which is based upon the solution for an inclined crack in a uniaxial tension field and an experimentally obtained fracture criterion for mixed mode crack configurations. Test results are presented for residual strengths of machined damage specimens to ascertain the statistical nature which arises from extreme damage detail, smooth holes and sharp cracks. Finally, probability of failure curves are given for both machined (7075-T6) and impact damage (7075-T6 and 2024-T81) in aluminum uniaxial tension panels.

Army Materials and Mechanics Research Center,
Watertown, Massachusetts 02172
PROBABILITY BASED FRACTURE MECHANICS FOR IMPACT PENETRATION DAMAGE - Thomas P. Rich, Peter G. Tracy, Louis R. Tramontozzi, Jiro Adachi, Milo Benicek, Alan H. Katz, and Wilbert J. Foster

AD____________

UNCLASSIFIED
UNLIMITED DISTRIBUTION

Key Words

Fracture
Probability
Impact

Technical Report AMMRC TR 78-24, June 1978, 24 pp - illus-tables, D/A Project 1L162105AH84
AMCMS Code 612105.H840011

This paper presents a new method for assessing the residual strength of structural components which have sustained impact penetration damage. The method is based upon the application of the Weibull probability density function to account for the significant scatter in residual strengths which result from the random nature of impact damage detail (cracks, holes, and spall surfaces). To measure the extent of an impact damage pattern, a new parameter is presented which is based upon the solution for an inclined crack in a uniaxial tension field and an experimentally obtained fracture criterion for mixed mode crack configurations. Test results are presented for residual strengths of machined damage specimens to ascertain the statistical nature which arises from extreme damage detail, smooth holes and sharp cracks. Finally, probability of failure curves are given for both machined (7075-T6) and impact damage (7075-T6 and 2024-T81) in aluminum uniaxial tension panels.